A Dual-Loop PI controller for a DC/DC Full-Bridge Power Converter with ZVS modulation

M.E. Hervas, S. Vazquez, *IEEE Member*, M. Reyes, *IEEE Student Member*,
J.M. Carrasco, *IEEE Member*, and E. Dominguez, *IEEE Member*
University of Seville
Avd. de los descubrimientos s/n
Seville 41092
SPAIN
ehervas@zipi.us.es

***Abstract*-The analysis and design of a zero voltage switching (ZVS) full bridge DC/DC converter control is discussed in this paper. The power converter is used to regulate the output dc voltage. With this objective, the control strategy presented here is designed based in the equations that describe the output current and output voltage dynamics. The proposed controller employs a dual-loop scheme implemented with two proportional-integral blocks. The performance of the controller is verified through several simulations, showing that the voltage at the dc-link is regulated to the desired reference value ensuring a correct operation of the selected topology.**

I. INTRODUCTION

DC/DC topologies based on high frequency transformers are widely known [1]. Nowadays the development of semiconductors (like IGBTs) makes the use of these topologies possible in higher power applications.

The presence of the transformer in the converter provides characteristic features:

1) Isolation: If the converter is grid connected, lower frequency isolation transformer is no longer needed on ac side. As frequency increases, the size of the transformer and its weight are reduced, as high frequency transformer is lighter and smaller than the ac side one.

2) Voltage ratio adjustment: This topology allows a wider operating range just dimensioning correctly the transformer.

The added complexity of this topology is that switching losses increase with the frequency. Due to this fact, soft switching techniques, like Zero Voltage Switching (ZVS) [2], must be applied if a competitive efficiency is desired.

Described advantages have encouraged the utilization of this topology in applications like aeronautics [3, 4] or automotive [5, 6], where size and weight are important issues. Moreover, most of the renewable energy sources operate as dc voltage sources. Fuel cells or photovoltaics provide low voltage but high current levels; so that, DC/DC converters are usually needed to adjust these electrical magnitudes to typical operational ranges [7, 8] and some storage systems also operate as dc systems. High frequency has also been considered in power distribution applications to replace classical 50Hz transformers reducing size and weight of them. In this case, power electronics is added where there was no necessary before, but power quality and voltage stability can be improved and other functionalities are added [9, 10].

This paper describes a control strategy for DC/DC resonant converter in order to regulate the output voltage. PWM phase-shift modulation is also applied. First of all, selected topology is explained. Then, control strategy is developed including detailed equations. ZVS modulation is also implemented. Finally, simulation results are shown and conclusions are obtained.

II. SYSTEM DESCRIPTION

The selected topology consists of a full bridge DC/DC power converter, as shown in Fig. 1. Full bridge DC/DC converters have been extensively discussed in the literature [11-14]. It is comprised of four primary side switches, a high frequency transformer and a half wave output rectifier.

The diode output rectifier at the center-tapped secondary only allows unidirectional power flow. This topology is typically used to connect fuel-cell and PV-generators [7, 8]. Other applications like chargers for the diesel generator set batteries [15] and power distribution applications [10] require DC/DC converters with only unidirectional power flow capability.

TABLE I

SYSTEM VARIABLES

Parameters	Description	Parameters	Description
V_{in}	Input voltage	D_A , D_B	Rectifier diodes
C_{in}	Primary dc link	V_N	Rectifier voltage
i_{in}	Input current	L_o	Output filter inductor
Q_1 - Q_4	IGBTs	i_L	Current through output inductor
D_{Q1} - D_{Q4}	Antiparallel diodes	i_c	Current across secondary dc link
V_p	Transformer voltage on primary side	i_o	Output current
i_p	Transformer primary side current	C_o	Secondary dc link
V_{S1},V_{S2}	Transformer voltages on secondary side	V_o	Output voltage
i_{S1},i_{S2}	Transformer secondary side currents		

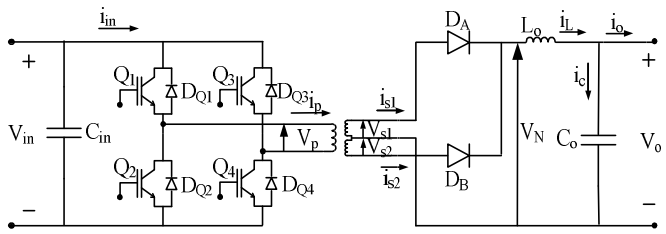

Fig. 1 Full Bridge DC/DC ZVS converter.

III. CONTROL STRATEGY

The main purpose of the full-bridge DC/DC control is to maintain the voltage across the dc-link at a defined value. This voltage should be maintained equal to the voltage reference value V_o^*. In this work, a dual-loop control scheme has been implemented. It consists of an inner current loop and an outer voltage-loop. Both controls have been implemented with a proportional-integral (PI) controller. Design of each controller will be described in this section in detail. The general scheme of the full bridge DC/DC control is shown in Fig. 2. In this figure, S represents the Duty Cycle of the inverter, V_o^* is the DC link voltage reference, i_L^* is the inductor current reference generated by the outer voltage control and r_T is the transformer turn ratio.

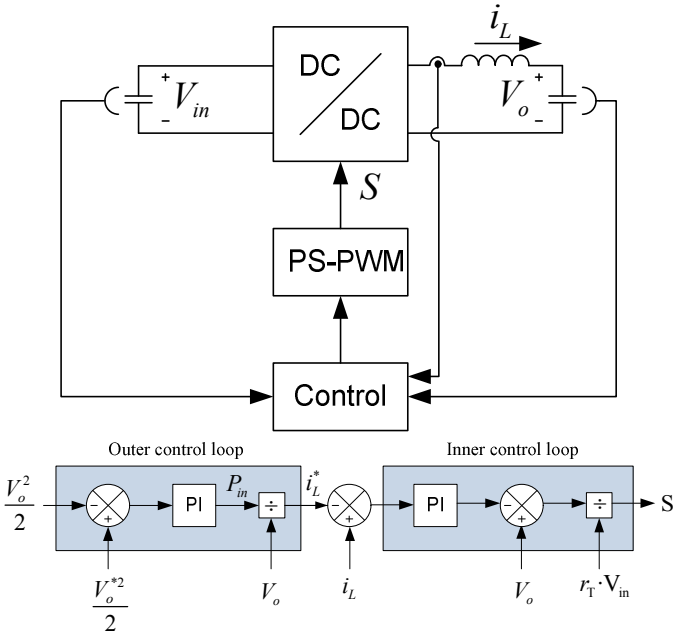

Fig. 2. Control strategy diagram block.

The voltage and current on the primary side depend on the inverter duty cycle.

$$V_p = S \cdot V_{in} \tag{1}$$

$$i_p = S \cdot i_{in} \tag{2}$$

where $S \in \{1, -1\}$.

The induced voltages in the secondary winding (V_{s1}, V_{s2}) are given by the input voltage and the transformer turn ratio.

$$V_{s1} = r_T \cdot V_p \tag{3}$$

$$V_{s2} = r_T \cdot V_p \tag{4}$$

The equations that describe the secondary side are,

$$V_N = r_o i_L + L_o \frac{di_L}{dt} + V_o \tag{5}$$

$$i_L = i_c + i_o \tag{6}$$

$$i_L = C \frac{dV_o}{dt} + i_o \tag{7}$$

In equation (5) the term $r_o i_L$ has been included to consider the voltage drop due to the Joule losses. Multiplying (7) by V_o,

$$V_o \cdot i_L = C \frac{d\left(V_o^2 / 2\right)}{dt} + V_o \cdot i_o \tag{8}$$

A. Outer voltage loop

The second term on the right hand side of equation (8) can be used to obtain the necessary input active power to regulate the dc-link voltage. To simplify the design process new variables are defined,

$$\theta \triangleq \frac{V_o^2}{2} \tag{9}$$

$$P_{in} \triangleq V_o \cdot i_L \tag{10}$$

$$P_o \triangleq V_o \cdot i_o \tag{11}$$

In equation (9) θ is the new input variable. P_{in} is the new control signal which represents the active power that system needs to maintain the dc voltage value. Introducing the variables θ, P_{in} and P_o, equation (8) is transformed in

$$P_{in} = C \frac{d\theta}{dt} + P_o \tag{12}$$

This equation corresponds to a LTI system, thus the value of P_{in} can be calculated like a PI controller [16]. For this purpose, the definitions of the input reference θ^* and input error $\tilde{\theta}$ are introduced.

$$\theta^* \triangleq \frac{V_o^{*2}}{2} \tag{13}$$

$$\tilde{\theta} \triangleq \theta - \theta^* \tag{14}$$

The implemented control with a proportional integral (PI) controller is presented in (15).

$$P_{in} = C \frac{d\theta}{dt} + P_o \pm C \frac{d\theta^*}{dt} \pm K_p \cdot \tilde{\theta} \tag{15}$$

By applying (14) to (15),

$$P_{in} = C \frac{d\tilde{\theta}}{dt} + K_p \cdot \tilde{\theta} + P_o - K_p \cdot \tilde{\theta} + C \frac{d\theta^*}{dt} \tag{16}$$

If the input active power is defined as

$$P_{in} \triangleq P_o - K_p \cdot \tilde{\theta} + C \frac{d\theta^*}{dt} \tag{17}$$

Consequently, the input error tends exponentially to zero,

$$0 = C\frac{d\tilde{\theta}}{dt} + K_p \cdot \tilde{\theta} \tag{18}$$

In steady state, the input reference θ^* is a constant value, thus its first derivative over the time is zero.

$$C\frac{d\theta^*}{dt} = 0 \tag{19}$$

Besides, in steady state the loads connected to dc-link can be considered constant. Under this assumption P_o can be regarded as an unknown constant perturbation that can be calculated using an integral term

$$P_o \triangleq -K_i \int \tilde{\theta} dt \tag{20}$$

Finally, the expression for the input control variable is

$$P_{in} = -K_i \int \tilde{\theta} dt - K_p \cdot \tilde{\theta} \tag{21}$$

where K_p and K_i are design parameters.
On the other hand, from (10) and (21) the reference current through the inductance will be given by

$$i_L^* = \frac{1}{V_o}(K_p(-\tilde{\theta}) + K_i \int (-\tilde{\theta}) dt) \tag{22}$$

A reference value of the current is given by the outer voltage loop. This value ensures that reference voltage across the dc-bus is achieved.

B. Inner current loop

The purpose of the inner loop is to guarantee current reference tracking, for this purpose the equation that represent the output current dynamic (7) is manipulated,

$$V_N = r_o i_L + L_o \frac{di_L}{dt} + V_o \pm L_o \frac{di_L^*}{dt} \pm K_p \cdot \tilde{i}_L \pm r_o i_L^* \tag{23}$$

The current error $\tilde{i}_L$ is defined as

$$\tilde{i}_L \triangleq i_L - i^*_L \tag{24}$$

By applying (24) to (23),

$$V_N = L_o \frac{d\tilde{i}_L}{dt} + (r_o + K_p) \cdot \tilde{i}_L + V_o + r_o i_L^* + L_o \frac{di_L^*}{dt} - K_p \cdot \tilde{i}_L \tag{25}$$

If the rectifier voltage V_N is given by,

$$V_N \triangleq V_o - K_p \cdot \tilde{i}_L + r_o i_L^* + L_o \frac{di_L^*}{dt} \tag{26}$$

Therefore, the current error tends to zero,

$$0 = L_o \frac{d\tilde{i}_L}{dt} + (r_o + K_p) \cdot \tilde{i}_L \tag{27}$$

On the other hand, the transformer voltage on the secondary side can be expressed as,

$$V_{s1} = r_T \cdot S \cdot V_{in} \tag{28}$$

At turn-on, diode can be considered an ideal switch because it turns on rapidly compared to the transients in the power circuit. Under this assumption V_{s1}=V_N and equation (26) can be redefined as follow

$$r_T \cdot S \cdot V_{in} = V_o - K_p \cdot \tilde{i}_L + r_o i_L^* + L_o \frac{di_L^*}{dt} \tag{29}$$

Using equation (29), equation (30) can be written as a function of the effective duty cycle,

$$S = \frac{1}{r_T \cdot V_{in}}(V_o - K_p \cdot \tilde{i}_L + r_o i_L^* + L_o \frac{di_L^*}{dt}) \tag{30}$$

Now, assuming that in steady state the load connected to the output dc-link is constant then i_L^* can be considered as a constant value yielding to

$$\frac{di_L^*}{dt} = 0 \tag{31}$$

Thus, the duty cycle can be calculated as

$$S = \frac{1}{r_T \cdot V_{in}}(V_o - K_p \cdot \tilde{i}_L + r_o i_L^*) \tag{32}$$

Besides, in steady state the joule losses can be considered constant. Under this assumption $r_o i_L$ can be regarded as an unknown constant perturbation that can be calculated using an integral term

$$r_o i_L^* \triangleq -K_{ic} \int \tilde{i_L} dt \tag{33}$$

Finally, the expression for the duty cycle is

$$S = \frac{1}{r_T \cdot V_{in}}(V_o - K_{pc} \cdot \tilde{i}_L - K_{ic} \int \tilde{i_L} dt) \tag{34}$$

where K_{pc} and K_{pi} are design positive parameters.

IV. MODULATION

Once the control signal S is obtained, a phase-shift control is implemented. The full-bridge converter with PWM phase-shift control achieves very high efficiency at high operating frequencies. The main concept in phase shift control is to vary the phase between two duty cycle control signals [17]. The output of the converter can be regulated by modulating the time when both diagonally opposite switches in the bridge are conducting simultaneously. This phase shift determines the operating duty cycle of the converter and it allows reduce the switching losses because bridge converter can be operated in soft switching mode. This control requires a complex four state PWM signal.

TABLE II

OPERATING STATES

State	ON	OFF
State 1	Q1, Q4	Q2, Q3
State 2	Q2, Q4	Q1, Q3
State 3	Q2, Q3	Q1, Q4
State 4	Q1, Q3	Q2, Q4

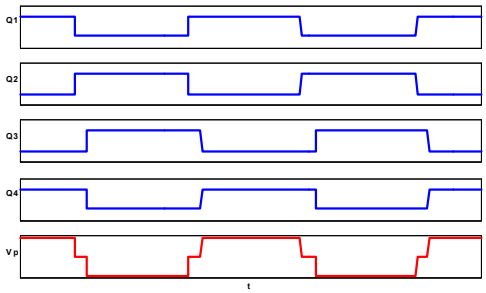

Fig. 3 PWM phase-shift waves

V. SIMULATION RESULTS

Resonant converters are applied in medium and low voltage power distribution applications. In order to decrease the semiconductor stress due to the voltage drop, a multilevel converter is introduced [18]. This converter is composed of 6 individual cells connected in series on the primary side. The topology presented in this paper consists on an individual cell of the multilevel converter. In this paper one of the mentioned cells is studied and a control scheme is proposed. To validate the proposed control scheme, digital simulations have been performed using PSCAD EMTC. The chosen parameters are shown in TABLE III, and resistive loads have been employed.

TABLE III

SYSTEM PARAMETERS

Parameter	Value
Primary DC link	2720 V
Electrical power rating	21 KVA
Transformer frequency	1 KHz
Output filter inductor	800 µH
Secondary DC link	700 V
Switching frequency	10 KHz

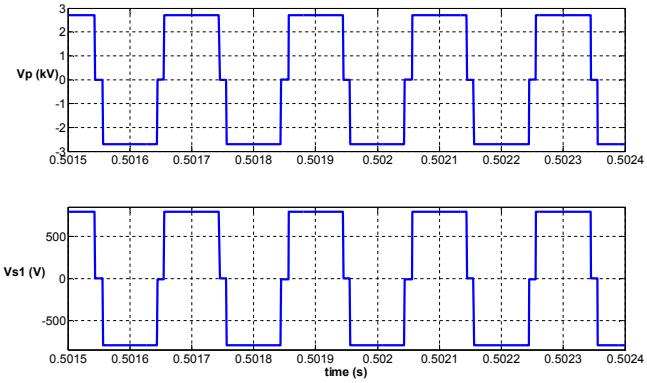

Fig. 4. Voltage V_p on primary side and voltage V_{s1} on secondary side

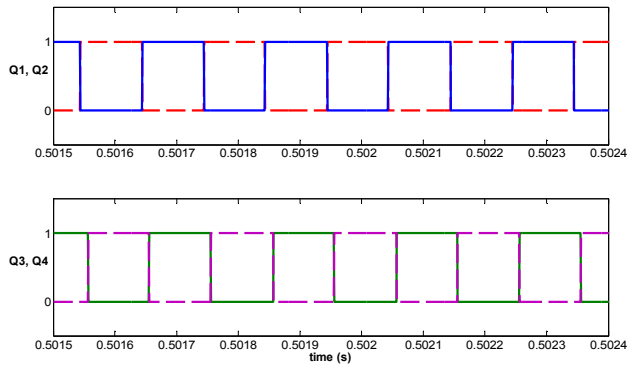

Fig. 5 IGBT's turn-on switching waveforms

Fig. 4, 5, 6 and 7 show the waveforms obtained during the simulation. Fig. 4 shows corresponding values for the transformer primary voltage V_p and the voltage on secondary side V_{s1}.

Fig. 5 depicts the gating of switches $Q_1 - Q_4$ and the phase shifted angle.

The transformer primary side current under zero voltage switching is maintained as shown Fig. 6. In Fig. 7, a detail of this current vs. voltage on primary side is shown.

The converter achieves high efficiency, typically 96.5% at 100% load. In terms of control characteristics Fig. 8 shows the output voltage depending on loading conditions. Above 0.5 seconds, load resistance varies from 35 to 25 ohms. Output voltage V_o decreases with an increase in load current. Immediately, system gives control to reach the reference voltage.

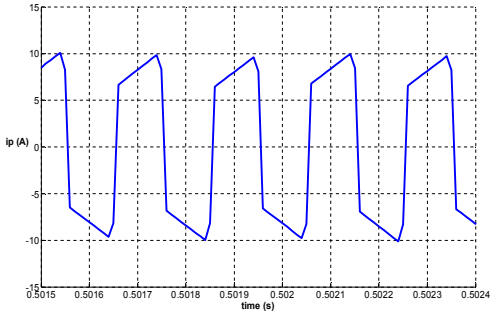

Fig. 6 Transformer primary side current

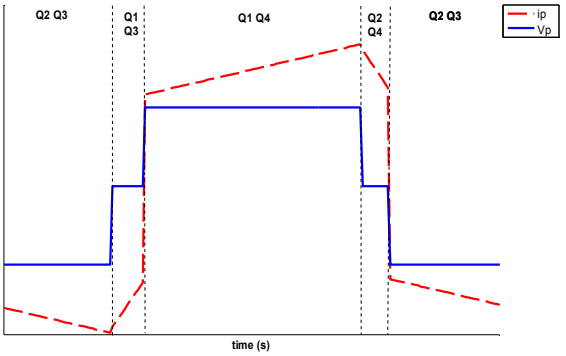

Fig. 7 Voltage and current through the semiconductors details

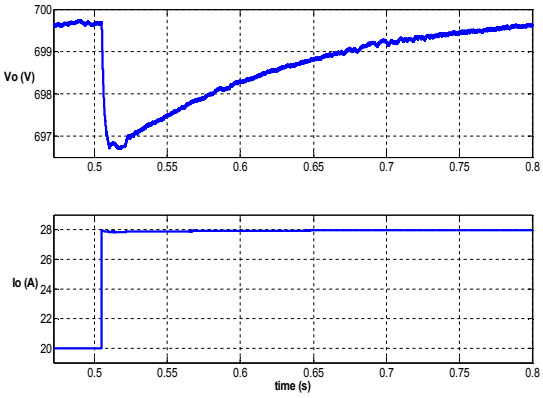

Fig. 8 Output voltage and output current depending on loading conditions

VI. CONCLUSIONS

In this paper, a novel control strategy for DC-DC Full Bridge converters is presented. A dual-loop control scheme has been proposed in order to deliver the desired power by means of tracking the corresponding output reference current and regulating the dc-link voltage at its output. Furthermore, switching losses are reduced using PWM Phase-Shift Control. Moreover, isolation is provided by the high frequency transformer. The proposed control method has been implemented and several simulations have been performed under different load conditions.

ACKNOWLEDGMENT

The authors gratefully acknowledge financial support provided by the Spanish Ministry of Science and Technology under project TEC2007-61879 and by the Andalusian Government Research Council under project P07-TIC-02991.

REFERENCES

[1] R. L. Steigerwald, R. W. De Doncker, M.H. Kheraluwala, "A Comparison of High-Power DC-DC Soft-Switched Converter Topologies", IEEE Transactions On Industry Applications, vol. 32, no.5, pp. 1139-1145, September/October 1996.

[2] S. Valtchev, B. V. Borges, and V. Anunciada, "1kW/250 kHz Full Bridge Zero Voltage Switched Phase Shift DC-DC Converter with Improved Efficiency" ,Telecommunications Energy Conference INTELEC '95, 17th International, pp. 803-807, October/November 1995.

[3] S. Aruselvi, T. Archana, G. Uma, "Design and implementation of CF-ZVS-QRC using analog resonant controller UC3861 for aerospace applications", Power System Technology, PowerCon 2004, vol.2, pp. 1270-1275, November 2004.

[4] P. Athalye, D. Maksimovic, R. Erickson, "High-performance front-end converter for avionics applications", Aerospace and Electronic Systems, vol. 39, pp. 462-270, April 2003.

[5] M. Pavlovsky, S.W.H. de Haan, J.A. Ferreira, "A ZVS, quasi-ZCS converter with an improved power rating for 14/42V automotive application", Power Electronics Specialist Conference, PESC '03, 2003 IEEE 34th Annual vol. 2, pp. 628-633, June 2003.

[6] A. Gorgerino, A. Guerra, D. Kinzer, J. Marcinkowski, "Comparison of High Voltage Switches in Automotive DC-DC Converter", Power Conversion Conference - Nagoya, PCC '07, pp.360-367, April 2007.

[7] K. Jin, X. Ruan, M. Yang, M. Xu, "A Novel Hybrid Fuel Cell Power System", Power Electronics Specialists Conference, PESC '06. 37th IEEE, pp.1-7, June 2006.

[8] G. Lefevre, B. V. Dang, J. P. Ferrieux, J. Barbaroux, Y. Lembeye, "New soft switching ZVS and ZCS half-bridge inductive DC-DC converters for fuel cell applications", International Power Electronics Congress, 10th IEEE, pp. 1-6, October 2006.

[9] G.T. Rado and H. Suhl, Eds. L. Heinemann, "An Actively Cooled High Power, High Frequency Transformer with High Insulation Capability", Applied Power Electronics Conference and Exposition APEC 2002, Seventeenth Annual IEEE, vol. 1, pp. 352-357, March 2002.

[10] T. A. Filchev, D. D. Yudov and V. V. Valchev, "Investigation of a DC-DC Resonant Converter For Power Distribution Applications", Electronics' 2004, September 2004.

[11] J. A. Sabaté, F.C.Y. Lee, "Offline application of the fixed-frequency clamped-mode series resonant converter", Power Electronics, Vol. 6, Pp. 39-47, January 1991.

[12] G. Hua, F. C. Lee, M. M. Jovanovic, "An Improved Full-Bridge Zero-Voltage-Switched PWM Converter Using a Saturable Inductor", IEEE Transactions on Power Electronics, Vol. 8, no. 4, pp. 530-533, October 1993.

[13] P. K. Jain, W. Kang, H. oin Y. Xi, "Analysis and Design Considerations of a Load and Line Independent Zero Voltage Switching Full Bridge DC/DC Converter Topology", IEEE Transactions on Power Electronics, Vol. 17, No. 5, pp. 649-657, September 2002.

[14] O. D. Patterson, D. M. Divan, "Pseudo-Resonant Full Bridge DC/DC Converter", IEEE Transactions on Power Electronics, Vol.6, No.4, pp. 671-678, October 1991.

[15] M. N. Gitau, G. Ebersohn, J. G. Kettleborough, "Power processor for interfacing battery storage system to 725 V DC bus", Energy Conversion and Management, Vol. 48, pp. 871-881, March 2007.

[16] G. Escobar, A. M. Stankovic, J. M. Carrasco, E. Galván, R. Ortega, "Analysis and design of direct power control (DPC) for a three phase synchronous rectifier via output regulation subspaces", IEEE Transactions on Power Electronics, vol. 18, no 3, pp. 823-830, May 2003.

[17] R. Redl, L.Balogh, D.W. Edwards, "Optimum ZVS Full-Bridge DC/DC Converter With PWM Phase-Shift Control: Analysis, Design Considerations and Experimental Results", Applied Power Electronics Conference and Exposition APEC '94, Conference Proceedings 1994, Ninth Annual, vol. 1, pp. 159-165, February 1994.

[18] L. Heinemann, "An actively cooled high power, high frequency transformer with high insulation capability", Applied Power Electronics Conference and Exposition, APEC 2002. Seventeenth Annual IEEE, vol. 1, pp. 352-357, March 2002.